Soft Matter

Cite this: *Soft Matter*, 2012, **8**, 360

www.rsc.org/softmatter

PAPER

Biofunctionalization of free-standing porous silicon films for self-assembly of photonic devices

Till Böcking,[abc] Kristopher A. Kilian,[a] Peter J. Reece,[b] Katharina Gaus,[c] Michael Gal[b] and J. Justin Gooding*[a]

Received 30th August 2011, Accepted 11th October 2011
DOI: 10.1039/c1sm06651j

Here we test chemical strategies for the fabrication of free-standing porous silicon thin films that are covalently modified on one of their faces with biorecognition elements to guide the vertical self-assembly of optical structures. Chemical modification *via* hydrosilylation of alkenes followed by coupling of biomolecules is carried out after the porous silicon film is lifted off from the silicon wafer to avoid damage to the organic monolayer during the lift-off step. Micron-sized biotinylated particles produced from asymmetrically modified porous silicon films are deposited *via* biorecognition in the correct orientation onto a substrate modified with avidin to form optical resonant microcavities.

Introduction

Porous silicon (PSi) is a versatile material suitable for the fabrication of a variety of photonic devices with applications including chemical sensors[1,2] and biosensors.[3–6] PSi is produced *via* electrochemical etching of silicon wafers in hydrofluoric acid containing electrolyte solutions, whereby the pore sizes and morphology can be tuned by varying parameters such as the doping level of the silicon substrate, the electrolyte composition and temperature.[7] Importantly, the porosity, *i.e.* the volume fraction of silicon removed during the etching process, depends on the applied current density. Since the porosity determines the refractive index of the material, one has the ability to precisely tune the refractive index profile normal of the surface simply by modulating the current density during the etching process, allowing the fabrication of high quality one-dimensional photonic crystals.[8–12] These photonic structures are typically a few μm thick and can be lifted off the underlying silicon substrate in a simple process to become free-standing films. After lift-off the PSi films can be fractured by sonication into micron sized PSi particles[13] with applications in microfluidics,[14–17] as spectral barcodes,[18,19] in drug delivery[20,21] and sensing at the cellular level.[22]

The key to fabricating PSi devices and particles lies in the choice of the surface chemistry used to impart the desired properties and functions.[23] The surface of freshly prepared PSi is terminated by silicon hydride species and is prone to oxidation in air resulting in a slow drift of the optical properties of the material.[23] This degradation is accelerated in aqueous environments where it can ultimately lead to dissolution and structural collapse.[24] Hence, one of the main challenges for fabricating biophotonic PSi devices is to passivate the PSi surface. This aim is most commonly achieved using self-assembled monolayers that also allow the introduction of functional groups for biorecognition and to resist non-specific adsorption of biomolecules. Hydrosilylation of unsaturated molecules (terminal alkenes and alkynes) has emerged as the most versatile approach for monolayer formation on hydride-terminated PSi *via* catalyzed, thermally induced and photochemical reactions.[25,26] Despite the wealth of literature in this area there is a continued need to develop and test chemical routes for the modification of PSi as applications of this versatile material emerge and are developed towards mature devices. In this context, surface chemistries are required to tune the stability of the PSi structure depending on its intended use. For example, PSi biosensors require high levels of passivation while a slow but continued degradation is necessary for drug delivery and release from PSi particles. Likewise different schemes are needed to introduce distinct functional groups onto the different surfaces of the PSi matrix including control over the modification on internal and external surfaces[27] or the preparation of asymmetric PSi films with different chemical functions on the top and bottom sides. The advantages and limitations of each route for derivatization also depend on the porosity, pore sizes, nanostructure and reactivity of the material, as well as on the compatibility with subsequent processing steps.

Here we investigate two approaches to produce and modify free-standing PSi films with carboxylic acid-terminated self-assembled monolayers *via* hydrosilylation of undecenoic acid followed by coupling of biomolecules. Asymmetric PSi particles biofunctionalized on their top surface are shown to assemble onto substrates in the correct orientation to form delicate optical devices, thus extending our recent method that utilizes biorecognition as the driving force for the assembly of optical structures into more complex architectures.[28]

[a]*School of Chemistry, University of New South Wales, Sydney, Australia. E-mail: justin.gooding@unsw.edu.au*
[b]*School of Physics, University of New South Wales, Sydney, Australia*
[c]*Centre for Vascular Research, University of New South Wales, Sydney, Australia*

Experimental

Etching of PSi Bragg reflectors and lift-off

Si(100) wafer pieces (p++, B-doped, 0.005 ohm cm, single side polished) were sonicated in ethanol (2 × 10 min) and acetone (2 × 10 min) and then blown dry under a stream of nitrogen. For PSi etching the wafer was placed onto a stainless steel back electrode in an electrochemical cell with platinum counter electrode and 25% ethanolic HF solution (mixture of 50% aqueous HF and 100% ethanol, 1 : 1, v/v) as electrolyte. The etching current density was modulated using a computer-controlled power supply to produce the alternating high and low porosity (low and high refractive index) layers. Etch stops were incorporated into the etching program to allow recovery of the electrolyte concentration at the dissolution front by diffusion. After etching the PSi sample was rinsed with ethanol followed by pentane and blown dry under a stream of nitrogen. To detach the PSi film from the Si substrate (before or after chemical modification) the sample was place into the electrochemical cell and subjected to a series of short high current density pulses using 15% ethanolic HF as electrolyte.

Monolayer formation on PSi

PSi Bragg reflectors were modified with monolayers *via* photochemical or thermally induced hydrosilylation of 10-undecenoic acid. The alkene was redistilled under reduced pressure before use. For the photochemical route the sample was covered with a thin film of the liquid alkene and placed into a quartz glass tube under a fast stream of argon. The tube was then connected to a bubbler and the argon stream was reduced. The sample was illuminated with a white light source (150 W halogen lamp) for 20 h while keeping the temperature slightly above 25 °C to avoid solidification of the alkene. Excessive heating of the sample was avoided by removing infrared radiation emitted from the lamp with a filter. After monolayer formation the sample was removed from the reaction vessel, rinsed with ethyl acetate and blown dry under a gentle stream of argon or nitrogen. For the thermal route a solution of undecenoic acid in mesitylene (1 : 2, v/v) was placed into a flame-dried flask and deoxygenated using four freeze-pump-thaw cycles before the PSi sample was placed into the solution under a stream of argon. The flask was then immersed in an oil bath heated to 120 °C and the reaction was allowed to proceed for over night. After alkylation the sample was cleaned as described above.

Biofunctionalization

The alkylated PSi sample was covered with a solution of 0.1 M NHS and 0.2 M EDC for 1 h to activate the carboxylic acid groups at the monolayer surface. Coupling of biomolecules to introduce biotin groups or to immobilize avidin was achieved by aminolysis of the NHS esters at neutral to slightly alkaline pH. Samples were biotinylated with a mixture of 1.7 mM (+)-biotinyl-3,6,9-trioxaundecanediamine (EZ-Link Amine-PEG3-Biotin, Pierce Biotechnology) and 3.3 mM 1-amino-hexa (ethylene oxide). Alternatively biotinylated bovine serum album was used for biotinylation.

Production of particles

After biofunctionalization the PSi film was released by breaking the edge connection of the film to the Si substrate. PSi particles were produced by sonication of the free-standing film in water using a bath sonicator.

Spectroscopy

Reflectivity spectra were measured at normal incidence over an area of 0.5 mm^2 by focusing monochromated light (J/Y SPEX 1681 spectrometer) onto the PSi sample and measuring the reflected light with a silicon detector. Transmission spectra of devices assembled *via* deposition of particles were measured by coupling the light collected with a microscope objective into an optical fibre for analysis using a spectrometer in conjunction with a CCD camera. The region of the sample for analysis was selected with an aperture (~140 μm in diameter). Microcavities assembled from particles could be tested with this set-up when the particles occupied at least ~half of the region selected with the aperture.

Results and discussion

The schemes for fabrication of a chemically modified, free-standing PSi film are shown in Fig. 1. In the first step a one-dimensional PSi photonic band-gap film is produced using electrochemical etching of Si(100), whereby a modulation of the

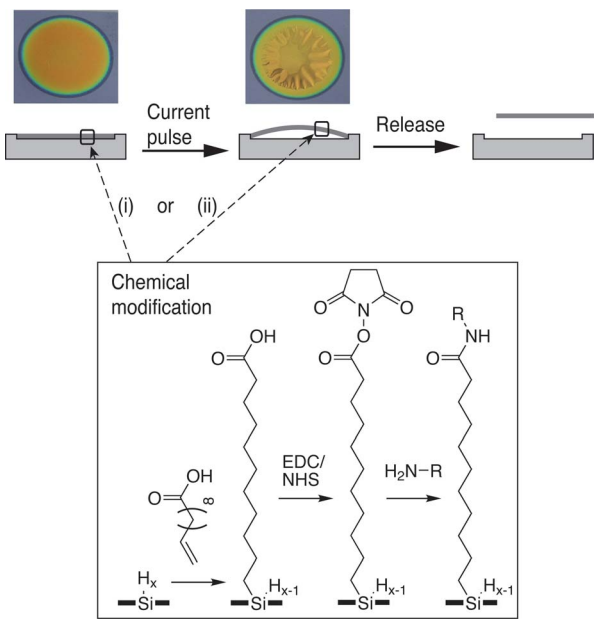

Fig. 1 Fabrication of chemically modified PSi lift-off films. Top: The PSi film fabricated by electrochemical etching is lifted off from the Si substrate by application of a high current pulse but remains attached to the substrate at its edges. The photographs show the PSi photonic crystal before and after application of the high current pulse. In the final step the modified PSi film is released from the substrate. Bottom: Chemical modification of the PSi can be carried out (i) before or (ii) after application of the high current pulse. Monolayer formation is achieved *via* hydrosilylation of undecenoic acid followed by standard coupling chemistries to attach biomolecules.

current density is employed to tune the porosity and hence the refractive index of the material normal to the surface. The photonic structure chosen for this work, a distributed Bragg reflector, is characterized by alternating layers of high and low refractive index and exhibits a band of high reflectivity in its optical spectrum bounded by low reflectivity interference fringes. At the end of the etching process the PSi film can be "lifted off" from the Si substrate by application of a high current pulse. The ~1.5 μm thick PSi film remains attached to its substrate at its edges resulting in a crumpled appearance of the PSi film as apparent from the photograph of the structure after lift-off (Fig. 1). Chemical modification of the PSi film can be carried out either before (approach (i)) or after the lift-off process (approach (ii)). In both approaches the hydride-terminated PSi is initially modified with a self-assembled monolayer *via* hydrosilylation of undecenoic acid followed by activation of the terminal carboxylic acid groups and coupling of biomolecules *via* aminolysis of the reactive N-hydroxysuccinimide ester groups on the monolayer. In the final step the modified PSi film is detached from the Si substrate at its edge and becomes completely free-standing.

Biofunctionalization of PSi Bragg reflectors before lift-off

To assess the utility of approach (i) in which the monolayer is formed before lift-off, as-prepared PSi Bragg reflectors were modified by photochemical[29–32] or thermal[33,34] hydrosilylation of undecenoic acid and further processed as outlined in Fig. 1. The chemical functionalization of the PSi structure was verified using FTIR spectroscopy in reflection mode (Fig. 2). The FTIR spectrum of a PSi Bragg reflector modified by white light-mediated hydrosilylation of undecenoic acid showed the absorptions characteristic of the carboxylic acid-terminated monolayer including the C–H stretching modes at 2918 cm^{-1} and the C=O stretch at 1718 cm^{-1}. The presence of unreacted silicon hydride species on the PSi surface was apparent from the peak at ~ 2090 cm^{-1} corresponding to the Si-H_x stretches. Further a broad peak at ~1100 cm^{-1} attributed to the Si-*O*-Si stretches revealed the formation of silicon oxide during monolayer formation. As generally observed for PSi thin films, the FTIR spectrum was dominated by an interference fringe arising from reflection at the air-PSi and PSi-Si interfaces. Subtraction of the interference fringe in the spectral regions diagnostic for the organic monolayer and silicon oxide facilitates comparison between samples and preparation methods. Fig. 3 shows that the level of oxide formation is considerable for monolayers prepared using white light-mediated hydrosilylation (shown in panel a) and those prepared using thermal methods (shown in panel b).†

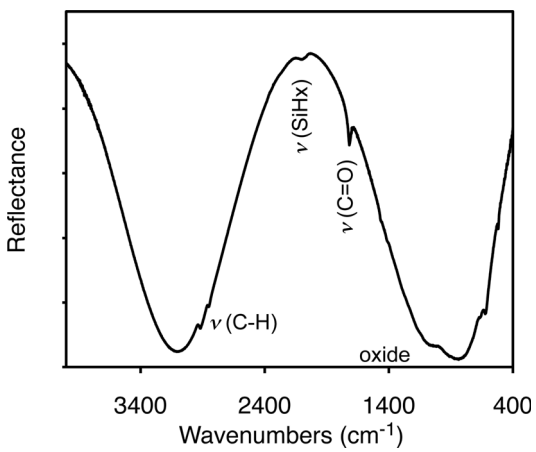

Fig. 2 FTIR spectrum of a PSi photonic crystal modified with an organic monolayer *via* white light-mediated reaction with undecenoic acid.

We utilized standard coupling chemistries for activation and immobilization of amines on the carboxylic acid-terminated monolayers. After treatment of the alkylated PSi with aqueous EDC/NHS the FTIR spectrum (Fig. 4) showed that activation of the terminal carboxylic acid group proceeded with high efficiency: The carbonyl stretch shifted from the value characteristic of the free acid (1718 cm^{-1}) to that characteristic of the NHS ester (1741 cm^{-1}). Further, absorbance bands arising from the NHS group appeared in the spectrum including those from the succinimidyl C=O groups at 1787 cm^{-1} and 1814 cm^{-1}, the N–O group at 1211 cm^{-1} and the C–O group at 1075 cm^{-1}. Finally the activated monolayer was biofunctionalized by reaction with a mixture containing a biotinylation reagent with an aminated hydrophilic spacer and a 1-amino-hexa(ethylene oxide) reagent to render the surface inert against non-specific adsorption of biomolecules. FTIR spectroscopy revealed the successful coupling of the reagents *via* aminolysis of the NHS esters as evident from the reduction of the peaks characteristic of the activated monolayer and appearance of the amide I and II bands

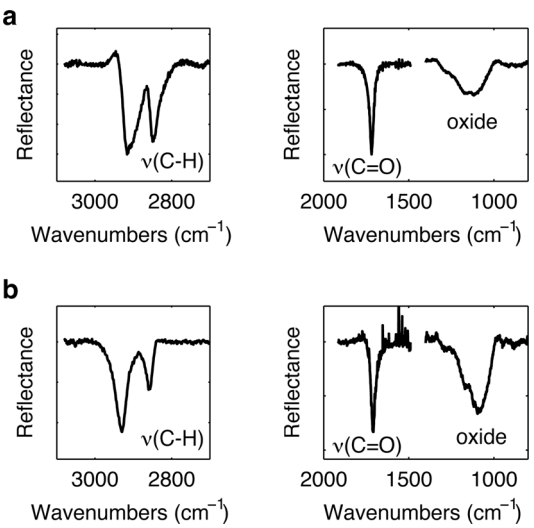

Fig. 3 Background corrected FTIR spectra of PSi photonic crystals after modification with an organic monolayer *via* (a) white light mediated or (b) thermal hydrosilylation of the hydride-terminated substrate with undecenoic acid. The spectra show the regions with peaks characteristic of the monolayer and of silicon oxide.

† We found that the oxide content of the modified Bragg reflectors etched from highly-doped Si was consistently higher than those observed previously for the same monolayers formed on PSi rugate filters etched from medium-doped Si. The observed differences in oxide formation, presumably resulting from the presence of residual oxygen and water in the reaction mixture, may be related to the differences in the pore sizes and morphologies for these types of structures.

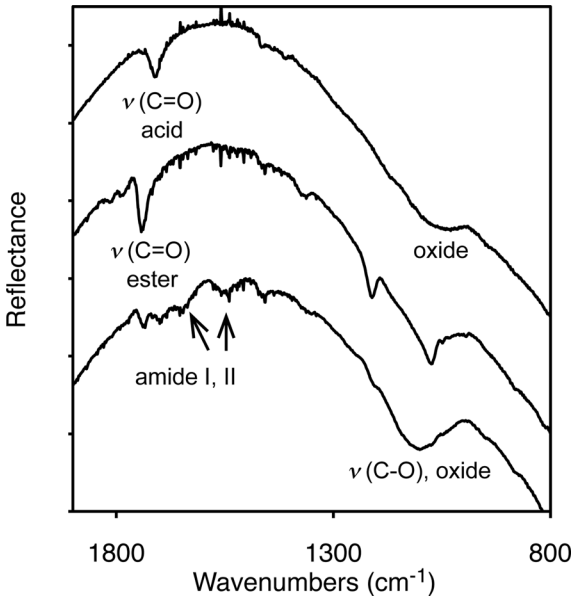

Fig. 4 FTIR spectra showing the stepwise derivatization of the PSi photonic crystal: COOH-terminated monolayer (top), after activation with EDC/NHS (middle) and after coupling of amines (bottom).

at 1650 cm^{-1} and 1548 cm^{-1}, respectively. The increase in the broad peak at ~1100 cm^{-1} was attributed to the C–O stretches from the ethylene oxide groups and presumably also included an increase in silicon oxide levels. Importantly, the PSi film remained structurally intact and showed no signs of the type of collapse that has been observed previously for other types of PSi photonic structures during modification.[24] This observation indicates that despite the oxide formation the coverage of the PSi surface with the organic monolayer is sufficiently high to stabilize the material.

The stepwise derivatization process was also evident from the optical reflectivity spectrum of the PSi Bragg reflector (Fig. 5). The spectral position of the Bragg plateau depends on the optical thickness of the alternating high and low porosity layers that make up the reflector. The optical thickness of a layer is given by the product of its refractive index, n, and its physical thickness, d. The Bragg reflectors in this study were designed such that according to the phase matching condition the centre of the photonic band gap, λ_0, is given by $\lambda_0/4 = n_H d_H = n_L d_L$, where n_H, n_L and d_H, d_L are the refractive indices and thicknesses of the high and low porosity layers, respectively. As the air inside the pores is partially replaced the organic material, the refractive indices of the layers increase and the Bragg plateau is shifted to higher wavelengths as a consequence. Fig. 5 shows the optical reflectivity spectra of the as-prepared Bragg reflector and of the same sample after successive steps the chemical modification. Monolayer formation resulted in the largest blue-shift of ~27 nm. Activation with aqueous EDC/NHS and biotinylation resulted in shifts of 7 nm and 14 nm, respectively, relative to the alkylated PSi photonic structure. The quality of the optical properties of the Bragg reflector did not degrade as a result of the surface treatments, which was further evidence that the monolayer sufficiently protected the PSi photonic crystal against structural break down under these conditions.

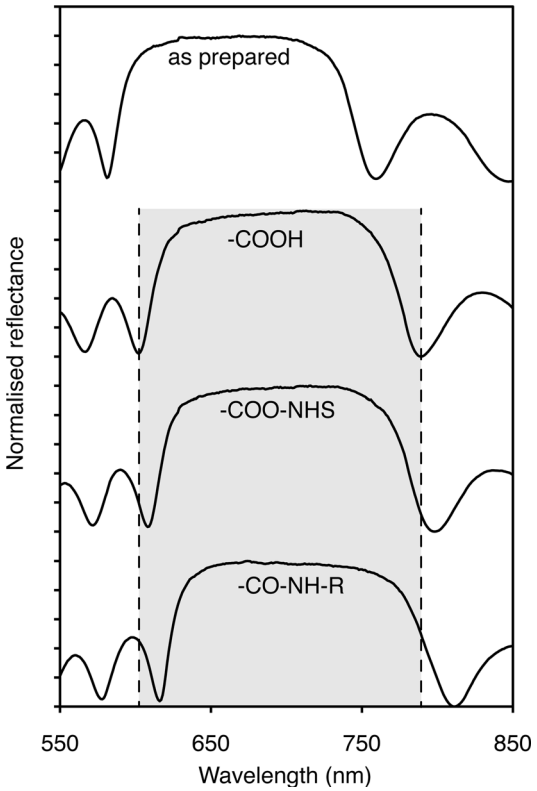

Fig. 5 Optical reflectivity spectra showing the stepwise derivatization of the PSi photonic crystal. The shaded region indicates the position of the Bragg plateau of the undecenoic acid-modified PSi photonic crystal to facilitate comparison with the subsequent modification steps.

Lift-off of functionalized PSi Bragg reflectors

The next steps in the fabrication process of approach (i) serve to detach the modified PSi structure from its Si substrate: The sample is immersed in an ethanolic solution of HF inside the electrochemical etching cell and subjected to a high current pulse. During this process, the PSi film is lifted off the Si substrate but remains attached to it at its edges. Modified PSi Bragg reflectors displayed a pronounced colour change after lift-off compared to the same samples before lift-off indicating that the process resulted in change of the refractive index of the material. This change was attributed to a partial dissolution of the porous matrix upon immersion in ethanolic HF. To assess the extent of the chemical and structural changes, a modified PSi Bragg reflector was immersed in ethanolic HF, rinsed, dried and analyzed by FTIR and optical reflection spectroscopy. The FTIR spectra in Fig. 6 show that the absorbances characteristic of the monolayer including the C–H stretches (see also insets of Fig. 6), C═O stretches and amide bands were greatly diminished after the etching step. Likewise the broad peak at ~1100 cm^{-1} was lost consistent with the removal of silicon oxide while the new absorbances at ~2090 cm^{-1} (Si-H_x stretches) and 660/618 cm^{-1} (SiH wagging/bending) revealed the reformation of a hydride-terminated surface. Thus, dissolution of the silicon oxide that had formed on the external and internal surface of the PSi matrix and presumably undergrown the organic monolayer resulted in a near complete loss of the organic material including the biotin

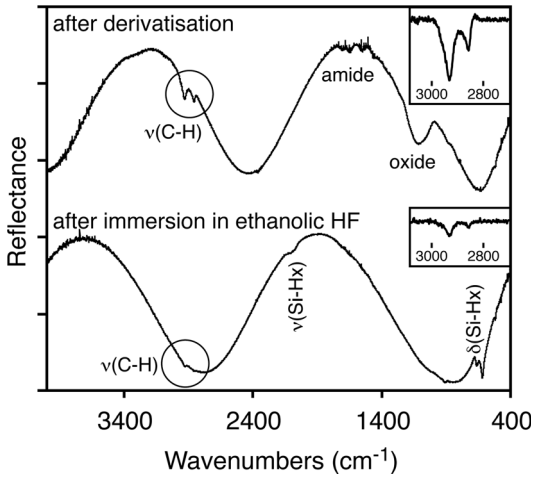

Fig. 6 FTIR spectra of a derivatized PSi photonic crystal before (top) and after (bottom) immersion in ethanolic HF. The insets show an expansion of the C–H stretches.

moieties at the surface of the device. The widening of the pores concomitant with the removal of the organic material and the oxide led to a decrease in the refractive index of the PSi layers and hence a pronounced red-shift of the Bragg plateau (*i.e.* the spectral window of high reflectivity) visible as a color change by eye and shown in the reflectivity measurements in Fig. 7. While derivatization led to an overall blue-shift of ~35 nm compared to the as-prepared structure, the etching step resulted in a pronounced red-shift of almost ~66 nm such that the central wavelength of the Bragg plateau was below that of the as-prepared structure as expected for the removal of the organic material and the oxide.

Biofunctionalization of PSi Bragg reflectors after lift-off

Since the oxide content of these structures led to the loss of the surface functionalization during the subsequent lift-off process, we investigated a second approach in which the order of these two steps was reversed, *i.e.* the PSi film was first lifted off (but remained attached to the substrate at its edges) and then chemically modified. PSi lift-off films were modified using light mediated hydrosilylation of undecenoic acid whereby the oxygen content was reduced by flowing a stream of inert gas over the PSi sample covered with a thin film of the liquid alkene prior to illumination. Fig. 8 shows the FTIR spectrum of a lift-off Bragg reflector modified in this fashion. The interference fringe was greatly reduced compared to the samples prepared by the first approach (*cf.* Fig. 2) because the PSi film is wrinkled and no longer flat against the substrate (see photograph of the sample after application of the current pulse in Fig. 1). The presence of the C–H and C=O stretches confirmed the successful formation of the carboxylic acid monolayer. As expected the photochemical reaction was dependent on the light intensity and the length of illumination. Judging from the intensity of the C=O stretch to the residual Si-H_x stretches, the reaction was about half complete after seven hours, >75% complete after 14 h and approached completion after 20 h of illumination. The long reaction time was attributed to the attenuation of light in the PSi structure due to scattering, absorption and reflection of wavelengths in the region of the high reflectivity band. Silicon oxide formation was observed as evident from the broad peak at ~1050 cm^{-1} arising from Si-*O*-Si stretching and the peak at ~2250 cm^{-1} due to OSi-H stretching, which results from migration to oxygen into the back-bonds of the silicon lattice. Nevertheless, the organic monolayer was sufficiently stable to prevent structural collapse of the PSi photonic crystal during subsequent coupling reactions in aqueous solutions. As a result, the number of biotin moieties introduced at the surface of the free-standing device using approach (ii) was considerably higher than observed for approach (i).

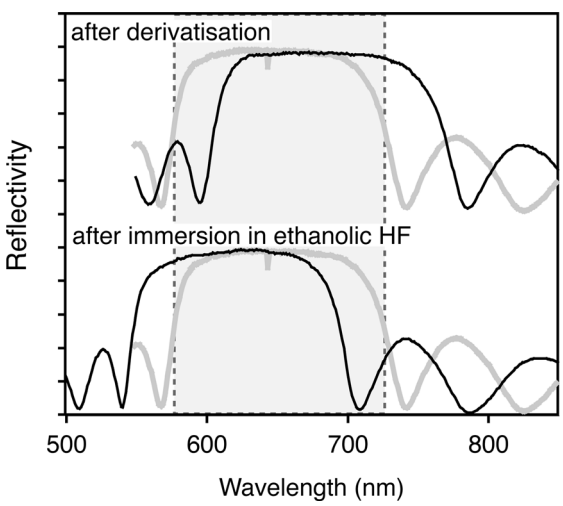

Fig. 7 Optical reflectivity spectra of a derivatized PSi photonic crystal before (top) and after (bottom) immersion in ethanolic HF. The spectrum of the as-prepared photonic crystal is shown for comparison in grey with the shaded area indicating the position of its Bragg plateau.

Self-assembly of optical devices *via* biorecognition

As a proof of principle for the utility of this approach for fabrication of asymmetrically modified and free-standing PSi films and particles, we chose to assemble optical resonant microcavities by depositing PSi particles in a controlled

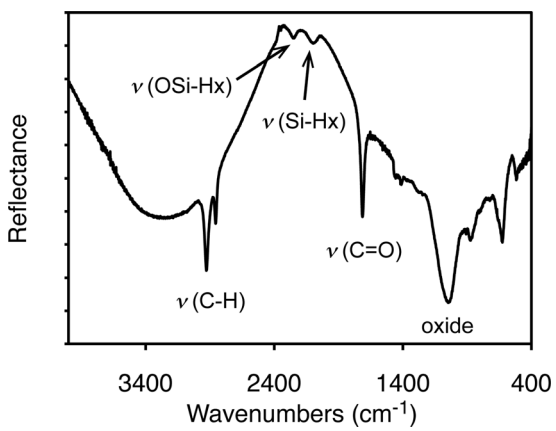

Fig. 8 FTIR spectrum of the detached PSi film after functionalization with an organic monolayer *via* white light mediated reaction with undecenoic acid.

orientation onto a PSi substrate, whereby the bonding was achieved *via* biorecognition. Optical resonant microcavities consist of two Bragg reflectors that are separated by a low refractive index spacer layer and are characterized by a resonance peak that appears in the Bragg plateau. The assembly approach is outlined in Fig. 9a: A lift-off Bragg mirror was bio-functionalized on its top surface with avidin while attached to the Si substrate,‡ released to become fully free-standing and then deposited onto a glass slide. A second PSi Bragg mirror was modified with avidin in the same fashion followed by bio-tinylated bovine serum albumin, released from the Si substrate and sonicated to produce irregularly shaped PSi particles with a thickness of ~1.5 μm and other dimensions typically in the order of 10^1–10^2 μm. Importantly, the top (biotinylated) side of the PSi Bragg mirror used for the particles contained a double thickness spacer layer. Biorecognition was then used to bind the particles *via* their biotinylated side to the avidin modified PSi Bragg mirror to form an optical resonant microcavity with the spacer layer etched as an integral part of the particle sandwiched between the two Bragg reflectors (see Fig. 9a). Conditions for the deposition of particles were not optimized such that only few particles bound to the substrate Bragg reflector in this pilot experiment. A photograph of such bound particles is shown in Fig. 9b. Microcavities are delicate devices that can easily be tested: A narrow cavity resonance peak only appears when the device is assembled in the correct orientation (*i.e. via* the biotinylated side) and with parallel alignment of the components to form a uniform spacer layer. To verify the formation of microcavities we measured the optical transmission spectra of the photonic structures (Fig. 9c): The transmission spectrum of the substrate Bragg reflector showed the Bragg plateau as a band of low transmission whereas the spectrum of the device deposited *via* biorecognition clearly showed the presence of the resonance peak at 668 nm thus confirming the successful assembly of a microcavity. The positions of the cavity resonance peaks measured for other particles ranged from 664 nm to 675 nm. These values were within the level of variation typically observed across the surface of the starting PSi structure (1 cm in diameter) and thus attributed to inhomogeneities arising from the electrochemical etching set-up. As discussed above only particles that are bound to the substrate *via* the biotinylated side will yield a cavity resonance. Most of the particles measured in this experiment exhibited a cavity resonance peak indicating that binding was specific and mediated by the biorecognition reaction.

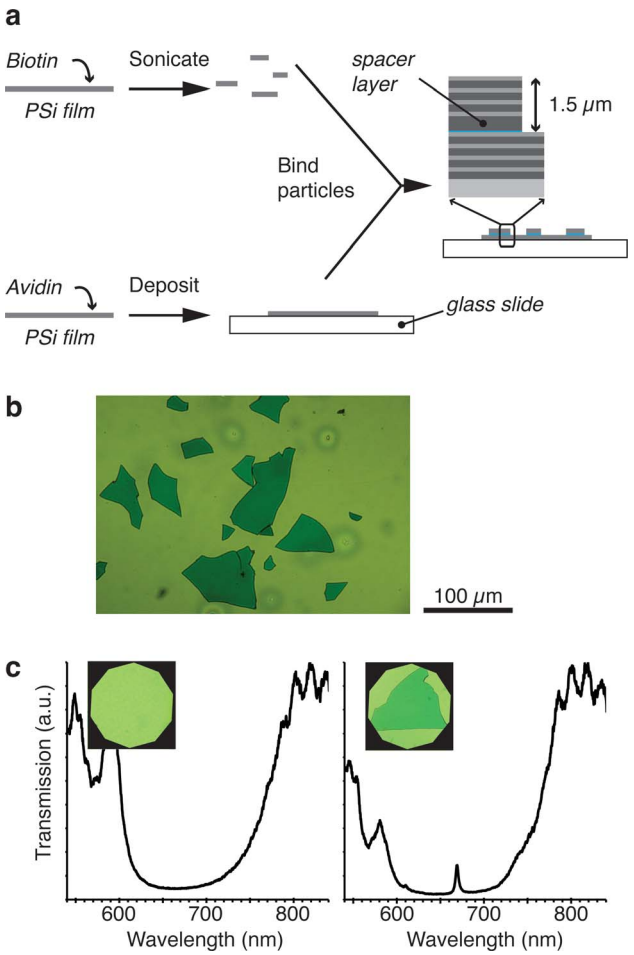

Fig. 9 Assembly of optical resonant microcavities *via* specific binding of biotin-functionalized PSi particles to a PSi Bragg mirror modified with avidin. a. Schematic representation of the assembly process. b. Photograph of PSi particles adhered to a Bragg mirror *via* biomolecular interaction between the biotin groups immobilized on the particle surface and the avidin immobilized on the substrate. c. Optical transmission spectra of the lift-off PSi Bragg mirror (left) and the microcavity formed by binding of a particle (right). The insets show the measured regions selected with an aperture.

The orientation-controlled deposition of particles onto substrates *via* biomolecules to assemble optical devices described here adds to the toolbox available in nanotechnology for the integration of components into more complex architectures.[35–37] We speculate that the ability to produce hybrid optical materials *via* vertical integration of layers opens up the possibility to fabricate biosensors with exquisite sensitivity, for example by incorporating a bioresponsive spacer layer into the microcavity. In this design the spacer layer could be laterally accessible to analytes, thus allowing to fabricate microcavities with presumed superior optical properties. Previous biosensor designs using monolithically grown PSi based microcavities require mirrors with large pores and low porosity contrast to allow diffusion of large analytes through the top Bragg mirror into the spacer layer with the drawback that pore enlargement leads to a degradation of the optical properties and hence the sensitivity of the device.[3] Optimisation of the particle deposition process from solution or from the solution-air interface may allow formation of dense particle monolayers[37] while deposition of different particles in different locations of the substrate could be achieved *via* surface patterning of biorecognition molecules.

Conclusion

In this work we have developed a strategy for the asymmetric biofunctionalization of free-standing PSi films and particles.

‡ The pore sizes of the low porosity layer prevent infiltration of the protein into the structure and hence the protein is largely confined to the top external surfaces of the PSi film.

Thermal and photochemical hydrosilylation of undecenoic acid on mesoporous silicon photonic crystals gave monolayers that sufficiently stabilized the PSi matrix in neutral aqueous solutions to allow activation of the terminal carboxylic acid groups and coupling of biomolecules. However, considerable oxide formation led to removal of the organic layer during a subsequent electrochemical lift-off step with HF as electrolyte. This problem was overcome by reversing the order of the processing steps, *i.e.* photochemical modification of the PSi film after lift-off with undecenoic acid followed by biomolecule immobilization and finally release of the asymmetrically modified PSi film from the Si substrate. The utility of this approach was demonstrated by the binding of biotinylated PSi particles to an avidin-modified PSi substrate to form delicate photonic structures thus extending the scope of our concept for the self-assembly of optical devices *via* biorecognition. The work also highlights the need to assess the advantages and disadvantages of chemical schemes to controlling surface properties in the context of the device design and its structural and chemical properties.

References

1 A. M. Ruminski, B. H. King, J. Salonen, J. L. Snyder and M. J. Sailor, *Adv. Funct. Mater.*, 2010, **20**, 2874–2883.
2 L. M. Bonanno and L. A. Delouise, *Adv. Funct. Mater.*, 2010, **20**, 573–578.
3 H. Ouyang, L. A. DeLouise, B. L. Miller and P. M. Fauchet, *Anal. Chem.*, 2007, **79**, 1502–1506.
4 F. Cunin, T. A. Schmedake, J. R. Link, Y. Y. Li, J. Koh, S. N. Bhatia and M. J. Sailor, *Nat. Mater.*, 2002, **1**, 39–41.
5 K. A. Kilian, L. M. H. Lai, A. Magenau, S. Cartland, T. Böcking, N. Di Girolamo, M. Gal, K. Gaus and J. J. Gooding, *Nano Lett.*, 2009, **9**, 2021–2025.
6 M. M. Orosco, C. Pacholski, G. M. Miskelly and M. J. Sailor, *Adv. Mater.*, 2006, **18**, 1393–1396.
7 H. Foell, M. Christophersen, J. Carstensen and G. Hasse, *Mater. Sci. Eng., R*, 2002, **39**, 93–141.
8 A. Bruyant, G. Lerondel, P. J. Reece and M. Gal, *Appl. Phys. Lett.*, 2003, **82**, 3227–3229.
9 S. Ilyas, T. Böcking, K. Kilian, P. J. Reece, J. Gooding, K. Gaus and M. Gal, *Opt. Mater.*, 2007, **29**, 619–622.
10 P. J. Reece, G. Lerondel, W. H. Zheng and M. Gal, *Appl. Phys. Lett.*, 2002, **81**, 4895–4897.
11 S. Chan and P. M. Fauchet, *Appl. Phys. Lett.*, 1999, **75**, 274–276.
12 S. Chan and P. M. Fauchet, *Proc. SPIE–Int. Soc. Opt. Eng.*, 1999, **3630**, 144–154.
13 J. L. Heinrich, C. L. Curtis, G. M. Credo, K. L. Kavanagh and M. J. Sailor, *Science*, 1992, **255**, 66–68.
14 J. R. Link and M. J. Sailor, *Proc. Natl. Acad. Sci. U. S. A.*, 2003, **100**, 10607–10610.
15 J. R. Dorvee, A. M. Derfus, S. N. Bhatia and M. J. Sailor, *Nat. Mater.*, 2004, **3**, 896–899.
16 J. R. Dorvee, M. J. Sailor and G. M. Miskelly, *Dalton Trans.*, 2008, 721–730.
17 J.-H. Park, A. M. Derfus, E. Segal, K. S. Vecchio, S. N. Bhatia and M. J. Sailor, *J. Am. Chem. Soc.*, 2006, **128**, 7938–7946.
18 S. O. Meade, M. S. Yoon, K. H. Ahn and M. J. Sailor, *Adv. Mater.*, 2004, **16**, 1811–1814.
19 S. O. Meade and M. J. Sailor, *Phys. Stat. Solidi*, 2007, **1**, R71–R73.
20 C. Park, J. Kim, S. Jang, H.-G. Woo, Y. C. Ko and H. Sohn, *J. Nanosci. Nanotechnol.*, 2010, **10**, 3375–3379.
21 E. C. Wu, J. S. Andrew, L. Cheng, W. R. Freeman, L. Pearson and M. J. Sailor, *Biomaterials*, 2011, **32**, 1957–1966.
22 B. Guan, A. Magenau, K. A. Kilian, S. Ciampi, K. Gaus, P. J. Reece and J. J. Gooding, *Faraday Discuss.*, 2011, **149**, 301.
23 K. A. Kilian, T. Böcking and J. J. Gooding, *Chem. Commun.*, 2009, 630–640.
24 T. Böcking, K. A. Kilian, K. Gaus and J. J. Gooding, *Adv. Funct. Mater.*, 2008, **18**, 3827–3833.
25 M. Stewart and J. Buriak, *Comments Inorg. Chem.*, 2002, **23**, 179–203.
26 J. M. Buriak, *Chem. Rev.*, 2002, **102**, 1271–1308.
27 K. A. Kilian, T. Böcking, K. Gaus and J. J. Gooding, *Angew. Chem., Int. Ed.*, 2008, **47**, 2697–2699.
28 T. Böcking, K. A. Kilian, P. J. Reece, K. Gaus, M. Gal and J. J. Gooding, *ACS Appl. Mater. Interfaces*, 2010, **2**, 3270–3275.
29 R. Voicu, R. Boukherroub, V. Bartzoka, T. Ward, J. T. C. Wojtyk and D. D. M. Wayner, *Langmuir*, 2004, **20**, 11713–11720.
30 Q. Y. Sun, L. C. de Smet, B. van Lagen, M. Giesbers, P. C. Thune, J. van Engelenburg, F. A. de Wolf, H. Zuilhof and E. J. Sudhölter, *J. Am. Chem. Soc.*, 2005, **127**, 2514–2523.
31 Q. Y. Sun, L. C. de Smet, B. van Lagen, A. Wright, H. Zuilhof and E. J. Sudhölter, *Angew. Chem., Int. Ed.*, 2004, **43**, 1352–1355.
32 F. Effenberger, G. Götz, B. Bidlingmaier and M. Wezstein, *Angew. Chem., Int. Ed.*, 1998, **37**, 2462–2464.
33 R. Boukherroub, J. Wojtyk, D. D. M. Wayner and D. J. Lockwood, *J. Electrochem. Soc.*, 2002, **149**, H59.
34 T. Böcking, E. L. S. Wong, M. James, J. A. Watson, C. L. Brown, T. C. Chilcott, K. D. Barrow and H. G. L. Coster, *Thin Solid Films*, 2006, **515**, 1857–1863.
35 E. Katz and I. Willner, *Angew. Chem., Int. Ed.*, 2004, **43**, 6042–6108.
36 A. Kulak, Y. Lee, Y. Park and K. Yoon, *Angew. Chem., Int. Ed.*, 2000, **39**, 950–953.
37 S. Y. Choi, Y. J. Lee, Y. S. Park, K. Ha and K. B. Yoon, *J. Am. Chem. Soc.*, 2000, **122**, 5201–5209.

